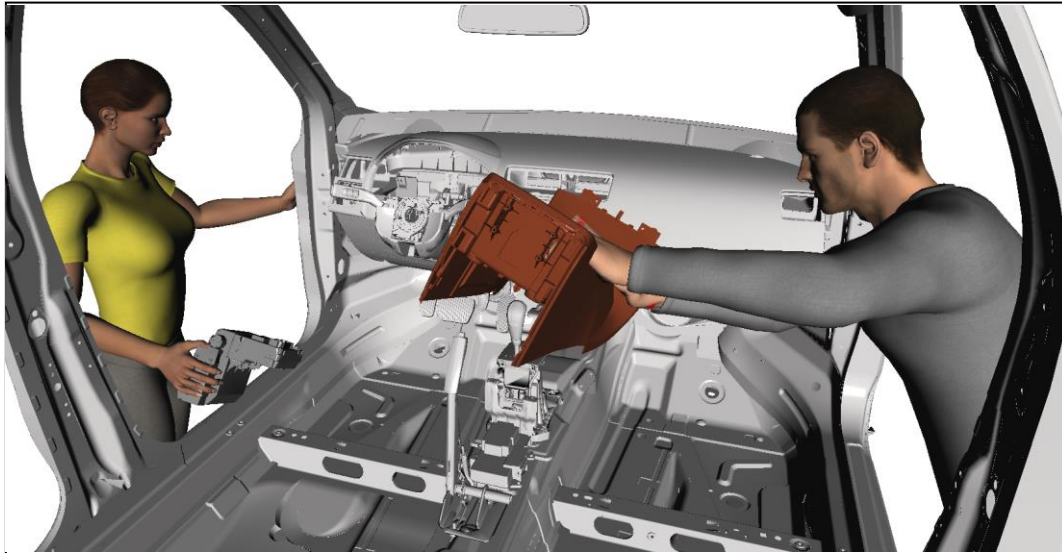# CHALMERS

Using Ergonomic Criteria to Adaptively Define Test Manikins for Assembly Operations

Master of Science Thesis in the Programme Computer Science: Algorithms, Languages and Logic

PETER MÅRDBERG

Using Ergonomic Criteria to Adaptively Define Test Manikins for Design Problems

Peter Mårdberg

Examiner: Peter Damaschke
Supervisor: Johan S Carlson

Chalmers University of Technology
University of Gothenburg
Department of Computer Science and Engineering
SE-412 96 Göteborg
Sweden
Telephone + 46 (0)31-772 1000

[Cover:
an explanatory caption for the (possible) cover picture
with page reference to detailed information in this essay.]

Department of Computer Science and Engineering

Göteborg, Sweden January 2014

ABSTRACT

Digital Human Modeling software is an important tool in virtual manufacturing that allows simulation of manual assembly work. Thus, it is possible to evaluate the ergonomics of the workers in an early stage of the development, long before any physical product has been built. Furthermore, it has also been shown that the ergonomics is related to the production quality, and is thereby an important factor to consider in order maintaining a sustainable high quality production.

In order to proper evaluate an assembly station, a set of manikins that are capture all the relevant ergonomic aspects has to be used. However, how to select these test manikins is a non-trivial task. This, since it is a tedious and time-consuming process to identifying which anthropometric variables that need to be considered in the assembly simulation.

When several anthropometric dimensions are considered, the designer must either use a set of predefined test manikins, or manually determine which anthropometric variables that should be used when the test manikins are generated. However, when a more complex assembly task is evaluated, how can the designer ensure that the test manikins accommodate the desired population? Or does there exist manikins that suffer from bad ergonomics even though all the tested manikins turned out well?

In this thesis, we propose a new algorithm for automatically building a set of test manikins called Adaptive Ergonomic Search (AES). Different manikins perform the assembly operation and the ergonomics is evaluated. The anthropometric variables that affect the ergonomics are identified and used to iteratively build up the set of test manikins. The algorithm considers the whole assembly operation and test manikins are generated from the entire set of anthropometric data. The algorithm has been compared with a percentile and to boundary methods on assembly cases from the automotive industry. The results shows that the AES algorithm generates test manikins that have worse ergonomics or may not be able to perform the assembly operation, than those manikins generated by the compared methods.

Keywords: Digital Human Modeling, Sampling Algorithm, Response Surface Method

ACKNOWLEDGEMENTS

TABLE OF CONTENTS

1 INTRODUCTION

Today in manufacturing industries, many parts of the production systems have been automated. However, there still exist a lot of manual assembly operations among the production lines. One reason to this is that a human assembly worker is very flexible and is therefore needed in the production when the production systems are too complex or expensive to automate.

In [4] the author shows a relation between the assembly ergonomics and the production quality, and concludes that the assembly ergonomics is an important factor to take into account in order to maintain a sustainable high quality production. Moreover, it is also important to consider this assembly ergonomics at an early stage, this since conceptual changes to products and assembly stations are less costly and easier to make if they are made early in the development [4, 5].

In a virtual environment it is possible to simulate a production system long before any physical prototypes have been built. Manikins represent human workers and are used to simulate manual assembly operations and make it possible to evaluate the ergonomics in an early stage of the development. However, to make these simulations useful, it is important to use test manikins that actually capture the ergonomic aspects in the assembly operation. A test manikin that captures some of the ergonomics in an assembly operation is hereafter denoted a relevant test manikin.

However, it is far from trivial to select relevant test manikins in order to properly evaluate an assembly operation. All the anthropometric dimensions that affect the design parameters have to be identified, which may require several advanced studies of the assembly operation. In some cases, there are only one or two design parameters that have to be considered. For instance, when testing the height of a chair or the height and width of a door, then it may be obvious which anthropometric dimensions that have to be investigated [6]. However, the task is far from trivial when several design parameters are involved [7, 6].

When multiple anthropometric variables are considered there exist two major strategies on how to select test manikins: distributed or boundary cases [7, 6]. However, neither of them takes the assembly operation in consideration when constructing test manikins, instead they assume that the same test set will be relevant for every assembly operation. When the ergonomics is evaluated in a more complex assembly task, is it then true that the predetermined test manikins always cover all the cases? Or does there exist manikins that suffer from bad ergonomics even though all the tested manikins turned out well? For instance, consider the three different assembly operations shown Figure 1-Figure 3. Are all these assembly operations covered by the same set of test manikins? If not, which are the different anthropometric dimensions that need to be taken into consideration in each of the assembly cases?

Figure 1: Shows an assembly case where a tunnel bracket is placed inside a car.
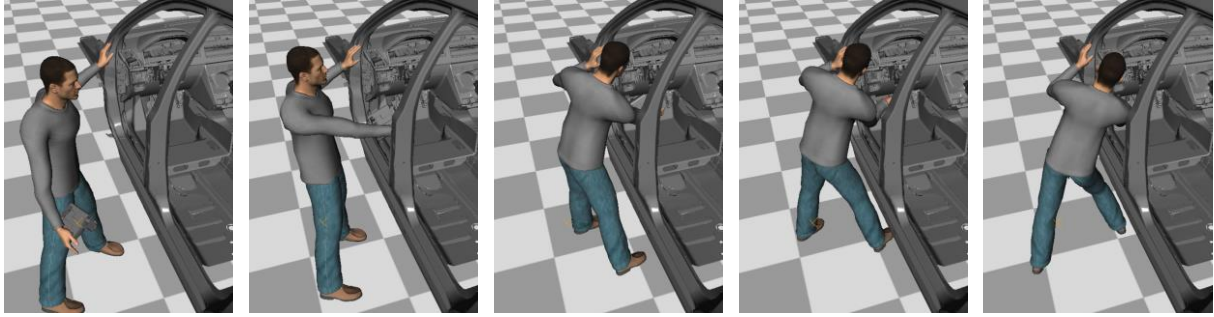
Figure 2: Shows the assembly of an electronic device inside the driving environment of a car.
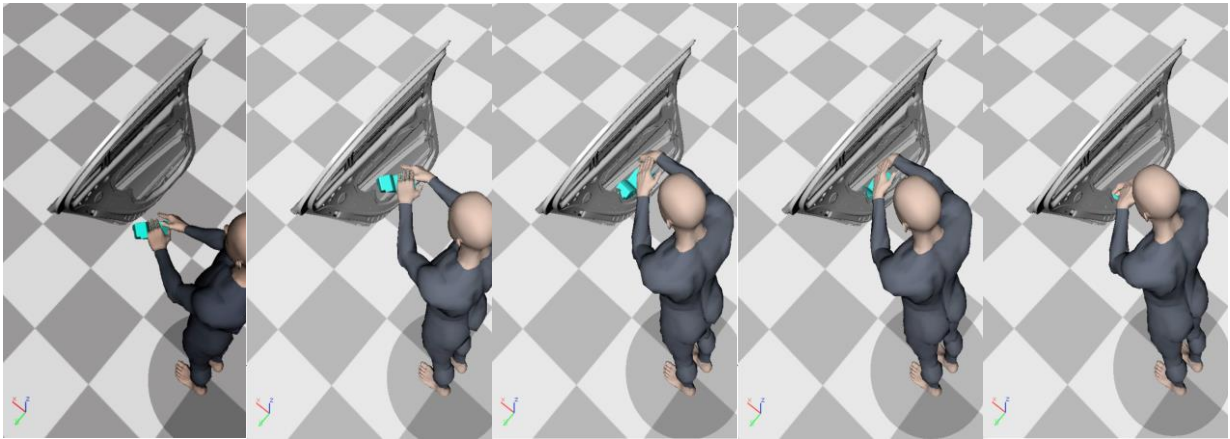
Figure 3: Shows the assembly of a protective block inside a car door.

In this thesis we propose a new algorithm for selecting relevant test manikins, called Adaptive Ergonomic Search (AES). The algorithm uses the whole set of anthropometric data to generate the relevant test manikins, and the ergonomics is considered throughout the entire assembly operation. The algorithm has been implemented in the Intelligently Moving Manikins simulation software [8] and tested on assembly cases from the automotive industry.

The test manikins generated by the AES algorithm are compared to the test manikins generated from boundary methods. As a reference, the generated manikins are also compared against a percentile method, which is a method that is commonly is used in industry today. The results show that there exist cases where the AES algorithm finds test manikins that have worse ergonomics than the manikins generated by the other methods. Furthermore, the AES algorithm reveals anthropometric combinations/regions where it may not be possible for an assembly operator to perform the assembly operation.

1.1 Background and Related Work

Different strategies for selecting relevant test manikins have been proposed throughout the literature. This section covers the two major strategies when several anthropometric variables are considered, and the percentile method.

1.1.1 Boundary Manikins

Boundary manikins are defined to represent the extremes of the anthropometric diversity. The potential of using boundary manikins is shown in [9], where 17 representative test manikins are generated and achieve the same accommodation as a sample of 400 manikins.

2

However, the boundary cases only give answers to the ergonomics on the max and min of an interval, and it is assumed that the ergonomics of the interior in between the intervals will always be less critical than the result from those on the boundaries. Furthermore, it is even assumed that there will not exist any other critical manikins on the boundary that might yield a worse result than those sampled. Figure 4 and Figure 5 shows the samples of boundary manikins when two anthropometric variables are used.

Two frontier boundary methods have been used in this work and are explained during the remaining part of this section.

BOUNDARY METHOD A

As stated earlier, the method assumes that the extremes of the anthropometric diversity represents the humans with the worst ergonomic. The manikins are generated with hierarchical regression equations where the extremes of stature and weight are used as dependent variables [10]. However, the method allows additional anthropometrical dimensions to be used as dependent variables in the regression equations.

The boundary manikins are generated based on the reduced set Y and the scaled axes of the hyper-ellipsoid, see section 3.4 add 3.5 for details. If p variables are used, then $2p + 1$ manikins are created, two manikins for each variable and one in the center, see Figure 4 for a two dimensional example. The axes and the confidence region of the hyper-ellipsoid are constructed as in section 3.4.

Figure 4: Shows how boundary method A selects dependent variables in a two-dimensional confidence region. The variables are selected to represent the extremes of the anthropometric diversity. An additional manikin is also generated from the center of the ellipsoid.

BOUNDARY METHOD B

The boundary manikins are generated based on the reduced set Y and the scaled axes of the hyper-ellipsoid. A number of boundary test manikins are defined by following an experimental design schema [11]. A Central Composite Design is used which defines one central test case in addition to one axial test case on the end of each axes of the hyper-ellipsoid and one factorial test case on each corner of a hyper-rectangle that spans the biggest volume possible inside the hyper-ellipsoid, see Figure 5. The ratio between an axial point and a factorial point along an axis is defined by
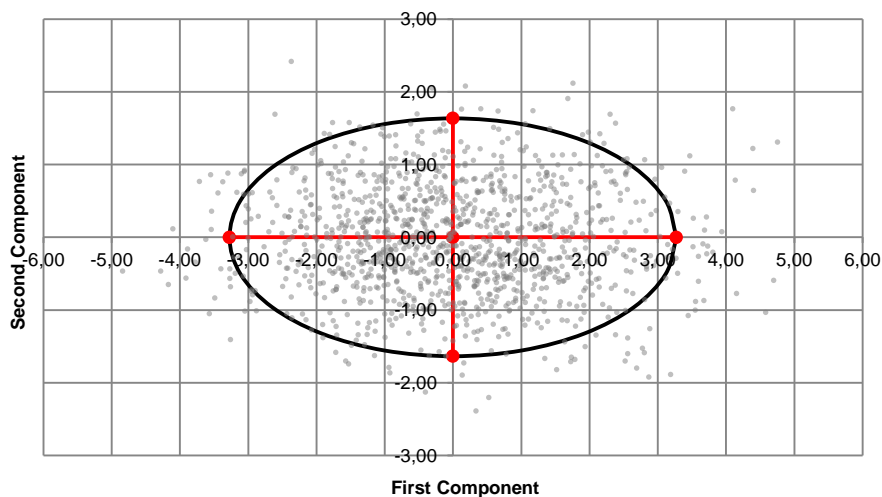
$$\alpha = \sqrt{p}$$

where p is the number of dimensions kept.
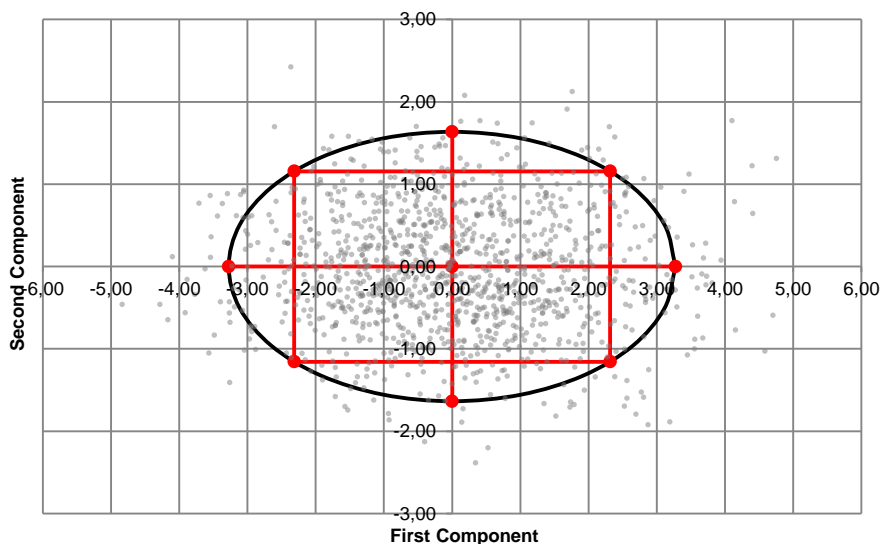
Figure 5: Shows how boundary method B selects dependent variables in a two-dimensional confidence region. The variables on the principal axes are selected to represent the extremes of the anthropometric diversity. Moreover, a manikin is also generated from the center of the ellipsoid and due to the Central Composite Design scheme, additional dependent variables are also selected at each corner of a hyper-rectangle spanned inside the hyper ellipsoid.

1.1.2 Distributed Manikins

The distributed test manikins can either be selected randomly or be predefined [7]. However, if a predefined set is used, will it then hold for the entire population in every simulation? Furthermore, when test manikins are selected by random sampling, how many samples have to be drawn to ensure that the desired region is covered?

An alternative distributed method is presented in [6]. It provides a typology from which the user builds up an appropriate set of test manikins. Each test manikin is defined from the stature, sitting height, and the waist circumference. Furthermore, the user may also specify anthropometric measurements that have to be taken into consideration. This way, it is possible to generate a sample that covers 82% of the population.

However, the Human Factors and Ergonomics Society [7] conclude that there is no automatic solution on how to choose any of these the distributed test manikins to ensure that the targeted population is accommodated.

1.1.3 Percentile Method

The percentile method is commonly used in the industry today and it is a method for selecting manikins due to one anthropometric dimension. Usually, the stature of a 5-percentile woman and a 95-percentile man are used to test if it is possible to perform the assembly operation in an ergonomic sound way.

The percentile manikins may be constructed in the same manner as the boundary manikins, see section 1.1.1. Thus, the percentile values may be extracted by projecting the reduced set onto the sought variable. An example is shown in Figure 6.
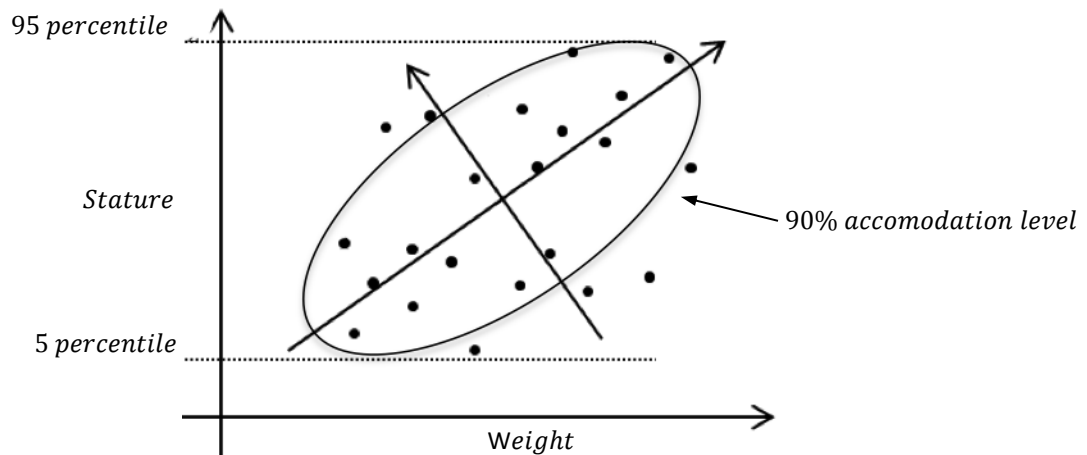
Figure 6: Shows an example on how the 5 and 95 percentile for stature may be extracted when the 2d ellipsoid accommodates 90% of the anthropometric data.

1.1.4 General About Generating Test Manikins

All the presented methods also rely on knowledge and experience of the users. For instance, a set of boundary manikins is defined from a set of anthropometric key dimensions that have been selected by the user. In [6], the user defines test manikins by using a typology. When random sampling is used, the user has to select the amount of samples. However, how can a user ensure that all necessary anthropometric dimensions are considered? Will different users define the same set of test manikins, or use the same number of samples?

1.2 Intelligently Moving Manikins (IMMA)

Digital human modeling software is used to create manikins. The software might either exist as a separate program or as a plugin to an existing CAD/CAE program. In this work, an independent manikin simulation software, Intelligently Moving Manikins (IMMA), have been used for both generating the test manikins and for simulating the assembly operations [8].

The manikin performs assembly operations by following pre-calculated collision free assembly paths. Figure 7 shows how a tunnel bracket may be assembled by following a pre-calculated assembly path. In this work, the collision free assembly paths are generated in the Industrial Path Solutions (IPS) [12] path planner.

Moreover, there are some features in the IMMA software that are fundamental for the AES algorithm to work. During the assembly simulation, the manikin automatically maintains balance, avoids colliding with the environment and tries to stay in as comfortable position as possible when it automatically performs assembly operations [13]. Also, the program supports automatic generation and evaluation of batches of test manikins.
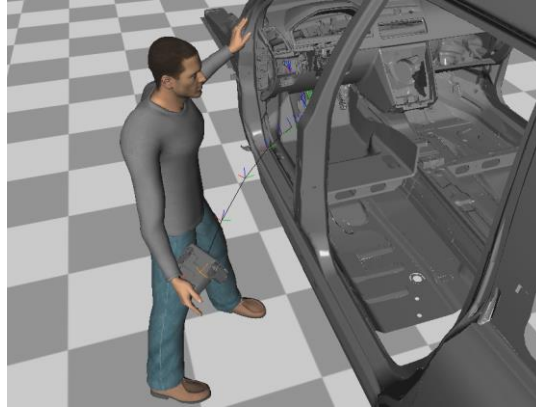
Figure 7: Shows how an electronic device is assembled by following a pre-calculated assembly path (the path is colored in green red and blue).

1.3 Scope and Limitation

The AES algorithm is a novel method for generating relevant test manikins, and the results are therefore compared to two boundary case methods that are frontier methods compared to what is used in industry today. Thus, as reference, it has also been compared with a percentile method.

To compare the AES with other methods for generating test manikins, and to make comparisons on even more complex assembly operations are considered as future work.

Moreover, there is no definition of what is considered as good or bad comfort in an assembly operation. In these experiments, the comfort for a manikin m that performs an assembly motion M is computed by a comfort function $c \to \mathbb{R}$, see section 3.3. We say that a manikin with $c(m, M) \gg c(m', M)$, has more discomfort when performing the assembly operation than the compared manikin m'. To define assessment methods to determine threshold values for good and bad comfort in terms of the comfort function is considered to be out of the scope of this thesis.

1.4 Outline of the Thesis

The thesis is structured as follows: Section 2 presents the methods used to accomplish this thesis. Section 3 presents the biomechanical model used in IMMA and the theory behind the developed AES algorithm. Section 4 presents the AES algorithm. The results of the algorithms are presented in Section 5, followed by a discussion in section 6. Section 7 contains the conclusions and future work.

2 METHOD

This section presents the research methods and the material that is used to accomplish the goal of the thesis.

2.1 Literature Review

A literature review was made in order to get a more in depth understanding in the area of assembly ergonomics. The major methods for generating test manikins were studied to understand the pros and cons of each method. Moreover, a literature study was also made to cover the underlying theory used in the AES algorithm.

2.2 Empirical Research

Empirical experiments were conducted to verify the theory that the major methods for generating test manikins may not cover all the manikins that have bad ergonomics when they perform an assembly operation.

2.3 Interview and Discussion

Discussions have been made with experts in the area of assembly ergonomics, ergonomic assessments and methods for generating test manikins Especially have discussion been made with PhD student Erik Brolin, Associate Professor Dan Högberg and Associate Professor Lars Hanson, see Appendix A for contact information.

2.4 Software Applications

The following programs have been used in this work, IMMA [8], IPS [12] and Visual Studio [14]. The code libraries that have been used are listed in Appendix A.

3 THEORY

This section covers both parts of the model that is used by the Intelligently Moving Manikins (IMMA) manikin and the underlying theory used by the Adaptive Ergonomic Search (AES) algorithm. The sections about the IMMA manikin show how the manikin is modeled and how the comfort for a manikin is defined. The sections with the AES algorithm show how the dimensionality of the anthropometric data set is reduced and the optimization methods that have been used.

3.1 Kinematical Model

The kinematical skeleton used in IMMA is a simplified model of the human skeleton, see Figure 8 a). The model is built out of links, where a link is an element that models the human joints and bones. A link is composed of a translation, rotation and a mass [15]. The translation is used to model the length of a human bone, whereas the rotation is used to model a human joint, see Figure 9. The mass represents the weight of the corresponding part of the body. More complex parts of the human body may be modeled by using several composed links. Hence, the freedom of a human joint that is allowed to rotate about more than one axis may be modeled by using several zero-length links. A one zero-length link is added for each axis too which the joint is allowed to rotate about [15]. For instance, the leg of the manikin is modeled using multiple links in different combinations. Since the human knee only rotates around one axis, it is sufficient to model the connection between the shin and the femur with only one link, whereas the human foot is more flexible and thereby modeled with multiple links. A composed and an exploded view of the links in the leg are shown in Figure 10 and Figure 11 respectively. The links are connected in a tree structure with the lower lumbar vertebra as root on the manikin. This root is connected to an external root, which is modeled to allow repositioning of the manikin [13], see Figure 8 a) and b).

In total, the kinematical skeleton is built up by 162 links, in which 82 links are used to model the human skeleton whereas the remaining model the freedom of the human joints. Each link in the kinematical model corresponds to one Degree of Freedom (DOF). The manikin has 162 DOF in total and is operating in $SE^3 = \mathbb{R}^3 \times SO^3$ [3]. Six DOF are needed to determine a position of in SE^3, three variables for the space coordinates of the manikin in $\mathbb{R}^3$, and three for describing the manikin rotation for each coordinate axis in SO^3.
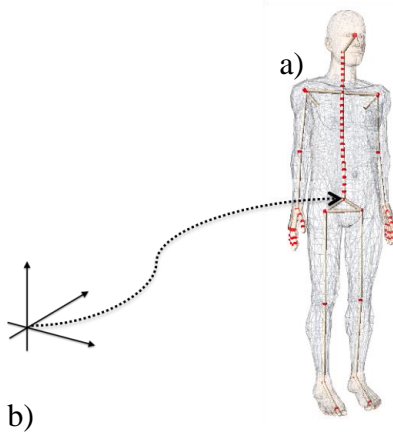
Figure 8: a) The kinematical skeleton of the manikin is shown under a transparent skin mesh. b) The external root that allows the complete manikin to be repositioned.
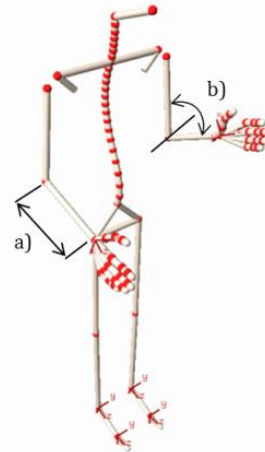
Figure 9: The kinematical skeleton is built up with links. A link is composed of a) a translation and b) a rotation. The rotation models the ability for the joint to rotate whereas the translation models the human bone.

Figure 10: A close up of a leg in the manikin skeleton. The knee rotates around one axis, while the foot rotates around three.

Figure 11: An exploded view of the leg in Figure 10. The knee is modeled with one link connecting the shin to the femur. Three links are used to model the ankle, in which two zero-length links are connected to the shin.

3.2 Kinematic Motions

Control frames, or as called in this work, Tool Centre Points (TCP) are used to place the manikin into the desired position, and they are typically defined at the hands and feet on the manikin, see Figure 9 a). Each TCP has a corresponding target frame TCP_{TARGET}. The manikin automatically tries to match its TCPs and the TCP_{TARGET}s. Hence, the manikin may automatically be repositioned by moving the TCP_{TARGET} to a desired position [15], see Figure 9 b). Several TCP's may be defined and each may have different rules. A rule defines how a TCP and a TCP_{TARGET} should match, see Figure 12, and a manikin is said to be in position if for each TCP matches the corresponding TCP_{TARGET} [15].
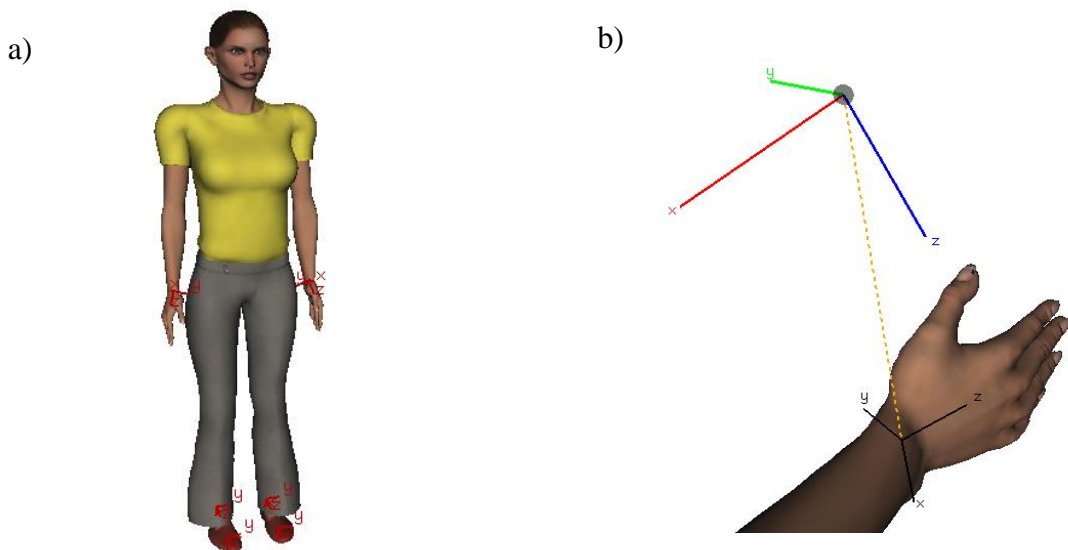
Figure 12: a) Shows the Tool Centre Points (TCP) on a manikin (marked in red). b) The manikin always tries to match the target Tool Centre Point TCP_{TARGET} (shown in red, green and blue).

10

Let $\theta = [\theta_1, \cdots, \theta_n]^T$ be the n dimensional joint angle vector which determines the position of the manikin. A movement of the manikin is defined as a sequence of poses. A set of m poses is called a motion, i.e. $M = \{\theta(t): t \in [1, m]\}$, where each pose represent a time step t in the assembly motion. Figure 13 shows a sequence of five poses sampled from a motion.
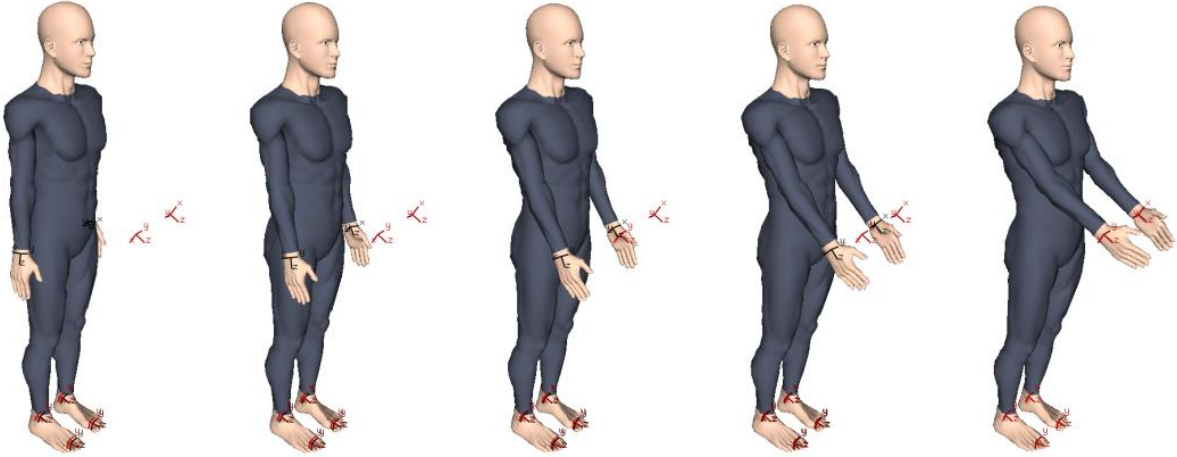
Figure 13: Five sampled poses of a manikin performing a motion.

For a position to be realistic it has to fulfill some rules. The manikin needs to maintain the balance while it holds the position. The balance has to consider the body parts and objects being carried, as well as exterior forces and torques in the environment. Furthermore, it also needs to avoid collision with objects in the environment. As stated in previous section, positioning of a manikin forms an underdetermined system. Thus, even if the assembly operation and human limitations adds more constraints to the system there exist an infinite number of ways of positioning the manikin in most cases [13]. A simple illustration of the impact of a redundant system with two degree of freedom is illustrated in Figure 14 whereas Figure 15 illustrates this redundancy in terms of manikins. However, the redundancy gives an opportunity to consider the ergonomic aspects by selecting the most comfortable of all the valid positions in each step of the assembly operation.
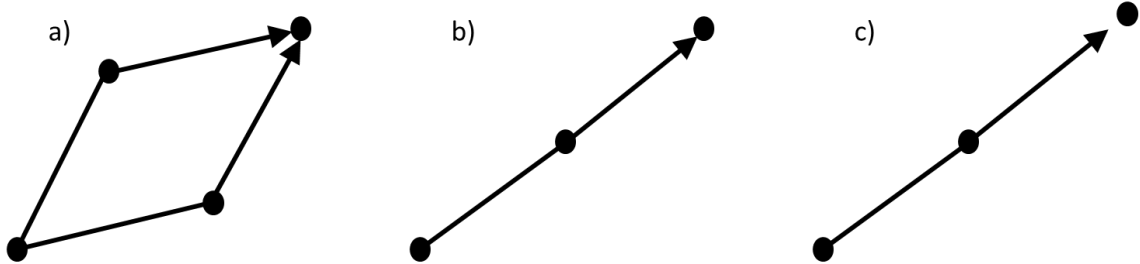
Figure 14: A kinematic system with two degrees of freedom, which has a) two solutions, b) one solution and c) no solution.
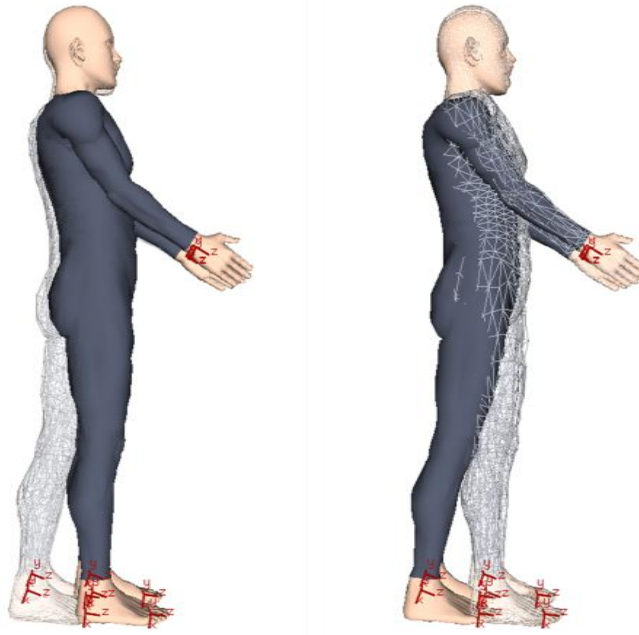
Figure 15: The redundancy of the system allow different body positions for the manikins, which in this case only are constrained to keep their hands in the same position and their feet on the floor. To highlight the difference, two manikins are placed onto each other, and the manikin with the skin mesh to the left is also shown with solid skin in the right side of the figure and vice versa.

3.3 Comfort Function

There exist infinitely many ways of positioning the manikin in most of the cases, see section 3.2, and this is used to consider the ergonomic aspects when the manikin performs an assembly operation.

The ergonomics in an assembly motion or position is, in the IMMA software, determined by the comfort function $c \rightarrow \mathbb{R}$, see Figure 16. It is defined to penalize high torques on the joints and poses where the joints are close to its limits. Thus, let M be the assembly motion for the manikin m, the comfort function for an assembly operation $\hat{c}$ is then defined as

$$\hat{c}(M,m) = \sum_{p \in M} c(p,m), \tag{1}$$

and the comfort for the manikin in position p as

$$c(p,m) = \left(\sum_{i=0}^{n} tan^2 \left(\frac{\theta_i \pi}{2 \theta_{max,i}} \right) + \sum_{i=0}^{n} w_i (\alpha_i T_i)^2 \right). \tag{2}$$

Where T_i is the torque, α_i is the rotational axis, and w_i a weight that defines the amount of allowed stress in joint i.

12
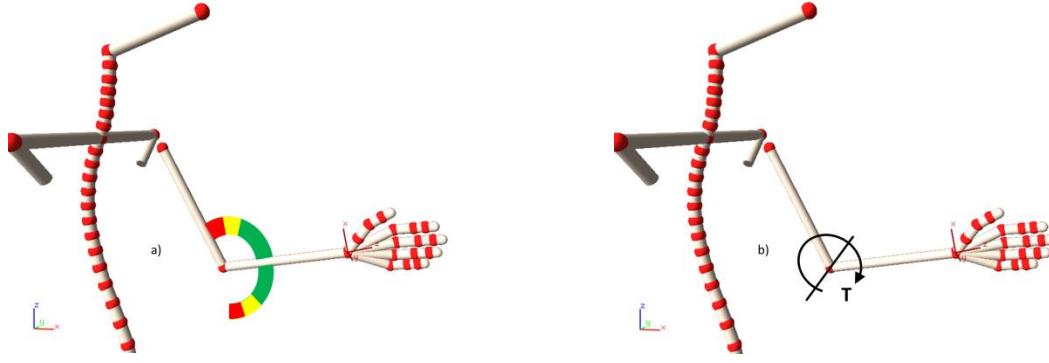
Figure 16: A joint is penalized when a) it is close to its end limits, and b) when there is a high torque on the joints.

3.4 The Anthropometric Data Set

The dimensions in the IMMA manikin are based on Swedish anthropometric data [16] The lengths of the links in the manikin are generated out of 56 anatomical variables, according to the ISO 7250 standard. However, due to missing data, only 39 of the variables are available. The missing data are estimated by using regression equations on additional data sets [17].

The dimensions in anatomical data sets are measured at the exterior of the human body, whereas the links in the manikin refers to internal body measurements, see Figure 17. The anatomical dimensions are transformed by regression equations to an internal dimension that may be used by the kinematical skeleton model [17].

When a large sample of anthropometric data is considered, it is valid to assume that it is normally distributed [18]. The normally multivariate distribution is denoted as

$$x \sim \mathcal{N}(\mu, \Sigma),$$ (3)

and the corresponding density function for k dimensions is defined as

$$f(x) = \frac{1}{(2\pi)^{k/2}|\Sigma|^{1/2}} exp\left(-\frac{1}{2}(x - \mu)^T \Sigma^{-1}(x - \mu)\right).$$ (4)

The density function only depends on x and is formed as a hyper-ellipsoid for a constant c [19]. The probability that an element is in the ellipsoid may be estimated using the chi-square distribution [19]. Hence, the confidence region for the anthropometric data set with dimensionality p and accommodation level ρ is given by

$$C_X = \left\{x: (x - \mu)^T \Sigma^{-1}(x - \mu) \le \chi_p^2(1 - \rho)\right\}.$$ (5)

The dimensionality of the hyper-ellipsoid is equivalent to the number of eigenvectors in Σ, and the length of the principal axes are determined by weighting the normalized eigenvectors with

$$k_i = \sqrt{\chi_p^2(1 - \rho)\lambda_i},$$ (6)

where p is the number of dimension kept and the ρ sought accommodation level.
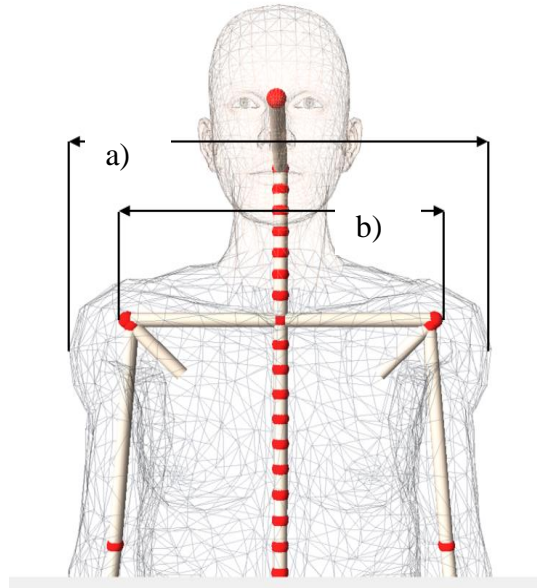
Figure 17: The anthropometric dimensions are measured at the exterior of the human body a), and the dimensions need to be adapted to the kinematical skeleton b).

3.5 Principal Component Analysis

Principal Component Analysis (PCA) is a dimension reduction technique that is suitable for normally distributed data sets [20]. PCA uses the dependent structures of the data and project it onto a lower dimensional space to capture the majority of the variance [20]. Thus, by studying the correlation among the variables it is possible to group the dependent variables. This is used to reduce the dimensionality of the data set by removing unrelated data from the original data set whereas the remaining data is used to create a new independent set.

Let X be a $n \times m$ data set where the rows corresponds to the n variables and the columns to the m samples, $\bar{x}$ the mean vector of X and let $S_m = \frac{1}{m}(X - \bar{x}')'(X - \bar{x}')$ denote the covariance matrix of X. Each ij'th element in matrix is the dot product of i'th and j'th with the j'th measurement type. The matrix is diagonal and symmetric, where the diagonal corresponds to the variance among the types and the off diagonal elements the covariance among the data set [20]. PCA creates a new orthogonal base, expressed as a linear combination of the original data elements. The new base is constructed such that the variance among the data is minimized [20]. This is shown in Figure 18. If the data set is normality distributed, then the linear transformation will represent the majority of the variance with the assumption that large values among the variance correspond to the important structure of the data [20].

Let a be a vector that captures the variance of X and let S_m denote the covariance matrix. The variance is maximized when the sum of squares is maximized as,

$$\max_a : a'S_m a,$$
$$s.t. \ a'a = 1,$$

(7)

The variance is maximized when a reaches infinity. Hence, a constraint $a'a = 1$ is defined to restrict the values of a [20]. Following the derivation of [20], the variance may be maximized subject to Eq. 7 by using a Lagrange multiplier for the constraint as,

$$a_1'S_m a_1 - \lambda(a_1'a_1 - 1).$$

(8)

14

Deriving the expression with respect to a and rearranging the formula we get,

$$\left(S_m - \lambda I_p\right)a_1. \tag{9}$$

From Eq. 8, it is shown that the eigenvectors of S_m are the vectors that maximize the variance. Furthermore, it is shown that ax is the first principal component of X. Thus, α_1 is the eigenvector corresponding to the largest eigenvalue λ in X. The following eigenvectors $\alpha_2 \cdots \alpha_n$ are constructed to capture the majority of the variance and are constrained to be orthogonal to the previous eigenvectors. This way, the eigenvectors spans a new orthogonal set where the majority of the variance is captured [20]. Moreover, the eigenvectors are constructed in a decreasing order due to the amount of accommodated variance.

Since the covariance matrix S_m and the correlation matrix P_X both are symmetric and quadratic matrices they may be decomposed as $S_m = A_{\Sigma_X} D_{\Sigma_X} A_{\Sigma_X}^T$ and $P_X = A_{C_X} D_{C_X} A_{C_X}^T$. Where A is an orthogonal matrix in which the columns are the eigenvectors of the decomposed matrix, and D is a diagonal matrix containing its eigenvalues.

The amount of variance captured by an eigenvector is given by

$$\frac{\lambda_i}{\sum_{i=1}^n \lambda_i}. \tag{10}$$

where λ_i is the i'th eigenvalue in D. Hence, to reduce the data set, select the first $p < n$ eigenvalues until a desired reduction ratio τ is reached as

$$\frac{\sum_{i=1}^p \lambda_i}{\sum_{i=1}^n \lambda_i} \geq \tau. \tag{11}$$

Let the remaining eigenvectors form a matrix A that may transform elements in the original set X onto elements in the reduced set Y. Figure 20 shows how the new orthogonal set Y captures the majority of the variance in the original set X. The column space of X is defined by A^T, which determines the possible outputs of any matrix.
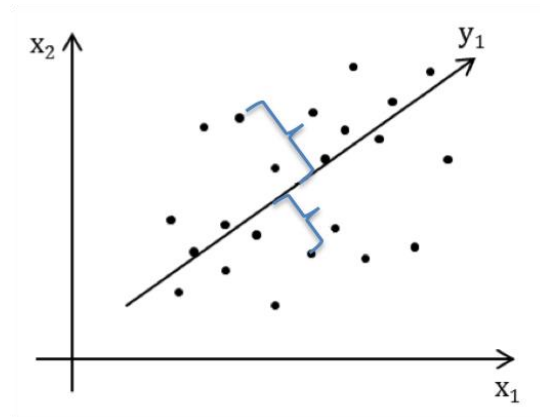
Figure 18: The new set Y constructed to minimize the variance in x. Hence, the first vector y_1, is constructed to minimize the orthogonal distance (two examples is marked with blue brackets) between the elements and the vector.
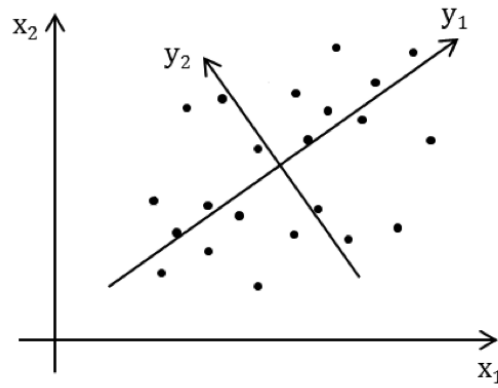
Figure 19: Eigenvectors are created to be orthogonal and to capture maximal variance of the underlying data. Hence, the second eigenvector y_2 is created both to capture maximal variance and simultaneously be orthogonal to y_1.
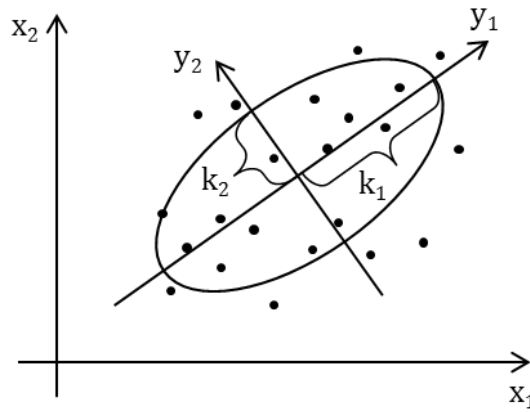
Figure 20: The 2D confidence ellipsoid of the new data set Y. The principal axes of the ellipsoid are defined by weighting y_1 with k_1 and y_2 with k_2.

3.6 Response Surface Methodology

Response surface methodology is commonly used in the field of experimental design to fit a mathematical model that describes the relation between the input and the yield of an unknown function [11]. The function is then used to improve a process or to evaluate the robustness of a system. In general, the system may be considered as a black box system where the input vector x yields a response y for a function as

$$y = f(x_1 \dots x_k) + \varepsilon_{Unknown}. \tag{12}$$

where $\varepsilon_{Unknown}$ is the noise of the error observed in y. The interaction with the underlying system may be identified by systematically perturbing the components of x. This way, it is possible to locally estimate a response surface of the unknown function f. However, since the true response function is unknown it may be the case that all inputs do not contribute to the response, and then it is possible to rule out those inputs and remove them from the approximated function [11]. However, it is assumed that all variables contribute to the model in the remainder of this section.

The choice of model for approximating an unknown function depends on the process studied and the region of interest. In many applications a lower order polynomial model, such as a first or second-order regression model is sufficient [11]. However, a higher-order model may be used in order to capture interaction among the variables [11]. A first-order linear regression model with k variables is defined as

16

$$y = \beta_0 + \beta_1 x_1 \cdots \beta_k x_k + \varepsilon, \tag{13}$$

where ε denotes the error in the model. The task is to estimate the regression coefficients β_i, which can be made by sampling f for different perturbations of x. Let $n > k$, and let n be the number of samples and k the number of coefficients. Written in matrix form we have

$$y = \begin{bmatrix} y_1 \\ \vdots \\ y_n \end{bmatrix}, x = \begin{bmatrix} 1 & x_{11} & \dots & x_{1k} \\ \vdots & & x_{ij} & \vdots \\ 1 & x_{n1} & \dots & x_{nk} \end{bmatrix}, \beta = \begin{bmatrix} \beta_0 \\ \vdots \\ \beta_k \end{bmatrix}, \varepsilon = \begin{bmatrix} \varepsilon_1 \\ \vdots \\ \varepsilon_n \end{bmatrix}. \tag{14}$$

The error is defined as the orthogonal distance between the sample and the estimated vector. To minimize the error is similar to minimizing the distance as shown in Figure 18. Hence, the best solution to the model is found by fitting a least square estimator $\hat{\beta}$, which serves as an estimate of the coefficient β and that minimizes the squared error. Thus we want to minimize

$$\varepsilon' \varepsilon = (y - X\beta)'(y - X\beta). \tag{15}$$

Deriving Eq. 14 with respect to $\hat{\beta}$ and rearranging the terms [11], $\hat{\beta}$ can be computed as

$$\hat{\beta} = (X'X)^{-1} X' y. \tag{16}$$

The quality of the estimated model may be shown by computing the R^2 value as

$$\beta' X' y - \frac{\left(\sum_{i=1}^n y_i\right)^2}{n} \bigg/ y' y - \frac{\left(\sum_{i=1}^n y_i\right)^2}{n}, \tag{17}$$

which corresponds to the quota of the regression sum of squares divided to the total sum of squares. An R^2 value close to 1 shows that the estimated model adequately fit the unknown function and that it captures the majority of the variation [11].

The choice of function to use as estimation for the unknown function also depends on the region which the approximated function is supposed to cover. A larger region may require a function with more variables, whereas a low order polynomial function might be sufficient if a smaller region is considered [11]. However, a larger region of the unknown function may be estimated by iteratively using low order polynomial functions to partially approximate the surface [11]. By letting the low order polynomial functions traverse the surface in the ascent or decent direction of the gradient as

$$x^{i+1} = \frac{\nabla y}{\|\nabla y\|} d + x^i, \tag{18}$$

where d is a unit step equal to the range of the sampled region covered by the estimated function, until optima of the unknown function is found.

3.7 Latin Hypercube Sampling (LHS)

Let f be an unknown function for which an estimate is sought. Moreover, assume that it is costly to evaluate f. Thus, it is desirable to try to estimate f by using as few samples as possible.

When samples are drawn randomly they are drawn from the cumulative distribution. However, many samples have to be drawn to identify the tails of the cumulative random distributions [21]. By drawing samples points uniformly from the experimental region it is possible to find a better estimate with fewer samples used. Such designs are called space-filling designs and are often used in experimental design to reduce the samples needed to estimate the unknown function [11].

A commonly used space filling method is Latin Hypercube Sampling [11]. By follow [21], a LHS may be constructed in the following manner. Scale each dimension to a unit interval, and let the unit interval for each dimension d be divided into K uniform regions. Moreover, let V_j^i for $i = 1, \cdots, d$ and $j = 1, \cdots, K$ be a uniform sample from the j'th region in the i'th dimension. Compose a d-tuple from the samples of each region j as $V_j^1, \dots, V_j^d$. Then each tuple represent a coordinate along the diagonal of a d dimensional hypercube.

Let π be a permutation of $\{1, \dots, K\}$ independently drawn from all $K!$, and with all permutations equally probable. Furthermore, let each $\pi_i(j)$ represent the mapping of the permuted coordinate j for the i'th dimension. Creating a new tuple as $V_{\pi_1(j)}^1, \dots, V_{\pi_d(j)}^d$, then the sampled regions are uniformly distributed over the dimensions of the unit cube and no longer restricted to the diagonal [21]. Figure 21 shows an example of a LHS with $K = 4$ and $d = 2$ together with the corresponding 2d-confidence ellipsoid.
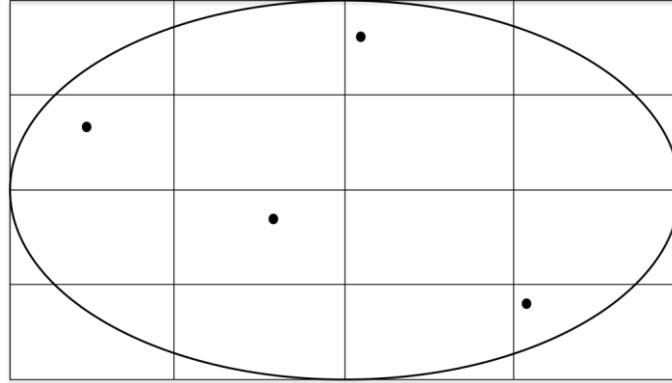
Figure 21: The LHS samples on a 2d grid together with a 2d confidence ellipsoid. The first and second principal axes of the ellipsoid give the length and width of the cube. Samples outside of the ellipsoid are discarded.

3.8 Constrained Optimization

This section shows how a constrained optimization problem may be formulated as an unconstrained optimization problem by expand the objective function to penalize violations to the constraints and then show how standard techniques for unconstrained optimization problems may be used solve the original problem.

A general constrained optimization problem may be formulated as

$$
\begin{aligned}
\min \quad & f(x) \\
s.t. \quad & g_1(x) \le 0 \\
& \vdots \\
& g_n(x) \le 0 \\
& h_1(x) = 0 \\
& \vdots \\
& h_n(x) = 0
\end{aligned}
\tag{19}
$$

The constraints $g_1, \cdots, g_n$ and $h_1, \cdots, h_n$, may be rewritten as a barrier function which favors points in the interior of the feasible region over those near the boundary [22]. A barrier function for g_i may be defined as

$$
\widetilde{g_i}(x) = \frac{-\mu}{g_i(x)},
\tag{20}
$$

where μ is a penalizing weight. Defining proper barrier functions from the all constraints and append them to f in Eq. 19, a new unconstrained optimization problem is constructed as

$$
\min \ f(x) + \widetilde{g_1}(x) + \cdots + \widetilde{g_n}(x) + \widetilde{h_1}(x) \cdots \widetilde{h_n}(x).
\tag{21}
$$

18

This may now be solved iteratively, as an unconstrained non-linear optimization problem where the penalty is reduced in each iteration [22]. Thus, in the first iteration a point p_I is selected in the feasible region. In the next step, let $\tilde{p}_B$ be the point found in the optimization. In the next iteration, set $\tilde{p}_B$ as starting point and decrease μ by a factor $\beta < 1$. Repeat until Eq. 21 converge [22]. Figure 22 illustrates how a barrier function blocks a non-valid region.
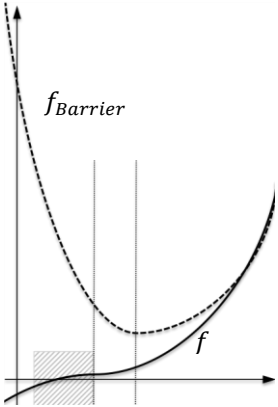
Figure 22: Shows a function with and without a barrier appended, denoted as f and $f_{Barrier}$ respectively. The barrier prevents the function from reaching a non-valid (dashed) region. However, $f_{Barrier}$ will reach the optima in f when the barrier penalty $\mu \to 0$ (The figure is adapted from [22]).

4 THE ADAPTIVE ERGONOMIC SEARCH (AES) ALGORITHM

This section first presents an outline of the AES algorithm whereas the following subsections then provide detailed information about each step of the algorithm.

4.1 Prerequisites for the Algorithm

As stated in section 1.7, there are some crucial prerequisites that a Digital Human Modeling (DHM) software needs to fulfill in order to use the AES algorithm. The manikins need to automatically be able to place themselves in the desired pose. Furthermore, it must also be possible to calculate the comfort in each pose. A manikin must always try to stay in as comfortable pose as possible and at the same time maintain the balance and avoid collision with objects in the environment. Moreover, the DHM software also needs to automatically handle the generation of manikin batches.

4.2 Outline of the Algorithm

In the preprocessing step, the data set is reduced according to the desired ratio, and a set of potential test manikins are then sampled from the confidence ellipsoid of this set. For each sample the algorithm locally estimates the comfort function and traverses it to find a manikin with worse ergonomic. These manikins are that have been found with the worst ergonomics is returned as test manikins to the user. Also, if a manikin fails to perform the assembly operation, the algorithm is aborted, and the manikin is returned to the user. The pseudo code of the algorithm is presented in Figure 23.

Preprocessing:

    1:   Calculate Σ, $\bar{x}$ and σ from the anthropometric data set X.

    2:   Reduce the dimensionality of Σ.

    3:   Create a set of samples S from the hyper-ellipsoid H.

Algorithm:

  Input: The set S of sample manikin.

  Output: The set T of local optimum test manikins.

     1:   For $m \in S$

     2:      If $c(m_{i+1})$ computes **then**

     3:         If $c(m_{i+1}) > c(m_i)$ **then**

     4:            If $m_{i+1} \in H$ **then**

     5:              Let $i := i + 1$

     6:              Let $m_{i+1} := \frac{\nabla c(m_i)}{\|\nabla c(m_i)\|} d + m_i$

     7:            Else

     8:              Let $m_{i+1} := \min_{m \in H} dist(m_{i+1}, m)$

     9:            EndIf

   10:         Else

   11:            Let $T := T \cup m_i$

   12:         EndIf

   13:      Else

   14:         Let $T := T \cup m_i$

   15:      EndIf

   16:   EndFor

   17:   Return T

Figure 23: The AES algorithm.

4.3 Preprocessing Step

Let X be the anthropometric data set. The rows of X correspond to the anthropometric dimensions whereas a column in X corresponds to a sample. Moreover, let C_X, σ and μ denote the correlation matrix, the standard deviation and the mean respectively.

By studying the correlation among the variables it is possible to group the dependent variables, which are used to reduce the dimensionality of the data set. Moreover, when the data set contains different dimensions of the measurements it might be more suitable to use the correlation matrix P_X instead since the big drawback of PCA based on covariance matrices is the sensitivity of the principal components to the units of measurement used for each element of X [20]. As stated in Section 3.4 the manikin is built out of 56 anthropometric variables. However, it is most likely the case that some of these variables do not have a major significance in the resulting comfort. By applying PCA on the correlation matrix P_X, it is possible to reduce the dimensionality of the anthropometric dataset and still maintain the majority of the human diversity. This, since the confidence region of normally distributed data is bound by a hyper-ellipsoid where the largest principal axes corresponds to the largest eigenvalues of the data set, see Sections 3.4 and 3.5.

Let $\widetilde{A}^T$ denote the matrix of eigenvectors kept after the reduction, and let an element $x \in X$ is be mapped onto the reduced set $y \in Y$ by a linear transformation as

$$y = \tilde{A}^T \left(\frac{x - \bar{x}}{\sqrt{\sigma}} \right). \tag{22}$$

The manikins are uniformly sampled throughout the entire set to increase the probability that all optima of the comfort function are found [23]. The samples S are drawn from the reduced set Y by using Latin Hypercube Sampling (LHS).

The confidence region of the anthropometric data set is bounded by a hyper-ellipsoid whereas the LHS draws samples from a hyper cube that covers the ellipsoid. Hence, samples may be selected from outside of the confidence region. However, these samples are discarded and resampled until all samples are within the hyper ellipsoid. Figure 21 shows how LHS samples are drawn from the hyper-ellipsoid with two variables.

4.4 Search Step

The sampled set S is considered to be potential relevant test manikins, and are used as seeds in the optimization process to identify the manikins with the worst ergonomic.

The comfort for a manikin that performs an assembly motion is determined by the comfort function. However, the comfort is calculated from the kinematical skeleton that is built out of data that has been adapted from the anthropometrical set. Also, the relevant test manikins are selected from a reduced linear combination of the original anthropometrical data set. Hence, there exist no one-to-one relation between the reduced anthropometrical data and the yield of the comfort function. To identify which anthropometric variables that affect the ergonomics in an assembly motion, the manikin is considered as a black box system. The inputs are the p reduced anthropometric variables in the reduced set Y and the comfort function is the system response

$$\hat{c}(M, y), \tag{23}$$

where M is the motion of an assembly operation.

A response surface is generated $\forall y \in S$, and each sample forms a local linear response surface using a first order polynomial function. Since the comfort function is differentiable in the interval of the joints, it can be used to identify the sensitivity of the influencing components in y^i for a motion M as

$$\nabla \hat{c}(M, y^i). \tag{24}$$

The response surface can be traversed by iteratively making local estimates of the comfort as

$$y^{i+1} = \frac{\nabla \hat{c}(M, y^i)}{\|\nabla \hat{c}(M, y^i)\|} d + y^i, \tag{25}$$

for a small step size d. The step size d also determines the region of the estimated surface. If the estimated model does not fit the underlying function well, d is iteratively reduced with a factor β. If $d < \varepsilon$, an optima has been

found.

As stated in section 3.4, the anthropometric data set is bounded by a hyper-ellipsoid that is sought to accommodate α% of the population. Hence, it might be the case that the manikin with the worst ergonomic may not exist within the hyper-ellipsoid. However, in these cases the algorithm tries to find the manikin on the boundary of the ellipsoid that has the worst ergonomic. Figure 24 shows how the algorithm follows the boundary of the ellipsoid and how it converges to a point that is orthogonal to the surface.

The boundary point may be found by minimizing the distance between the point inside the boundary and a point in the interior, see Figure 25. Let H be a hyper-ellipsoid and $p_O \notin H$. Let $p_I \in H$ be the point from which the algorithm stepped onto p_O. We now want to find a point $p_B \in H$ on the surface of the ellipsoid, which has the shortest distance relative p_O. The point on the surface p_B may be found by solving

$$min_{P_I}: \sqrt{(p_O - p_I)^2},$$
$$s.t. \quad p_I'Hp_I \leq 1. \tag{26}$$

The constraint ensures that p_B is inside the hyper ellipsoid. A constrained optimization problem may be formulated as an unconstrained optimization problem with a barrier function and then be solved as an unconstrained optimization problem, see Section 3.8. The constraint may be formulated as a barrier function,

$$g(p_I) = \frac{-\mu}{1-p_I Ep_I'}, \tag{27}$$

and by appending the $g(p_I)$ to the original object function Eq. 32, we get

$$min_{P_I}: \sqrt{(p_O - p_I)^2} + \frac{-\mu}{1-P_I'EP_I}. \tag{28}$$

In each step of the iteration, set p_I as start point and let $\tilde{p}_B$ be the point found in the optimization. In the next iteration set $\tilde{p}_B$ as starting point and decrease μ by a factor $\beta < 1$. The unconstrained optimization problem is in each iteration solved with a conjugated gradient method combined with a golden ratio line search.

The AES algorithm traverses the response surface in two ways. It either searches for the optima according to the ascent direction of the gradient, or it searches along the boundary of the allowed region, see Figure 24 a) and Figure 24 b) respectively. Thus, if there exist an optima on the boundary of the hyper ellipsoid, the algorithm starts to traverse the boundary until optima is found.

The optima that have been found corresponds to manikins that have the worst ergonomic when they perform the assembly operation. Thus, these manikins are returned to the user as relevant test manikins. Moreover, there may occur situations where the manikin cannot perform the assembly task. This may for instance be due to collision or reachability. If this occurs, the algorithm aborts the current search and returns the manikin that failed to perform the assembly operation as a relevant test manikin.
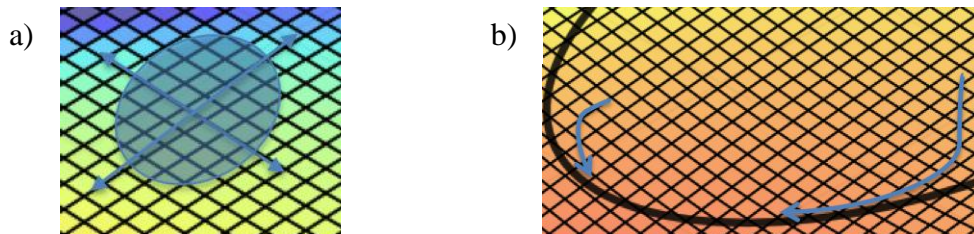
Figure 24: a) The ergonomics is locally identified (light blue region) in each sample point is and used to iteratively traverse the set until optima is found. b) The algorithm may follow the boundary until it converges to optima. The arrows indicate the path traversed on the estimated function where the discomfort increases, as the color gets more red.

24
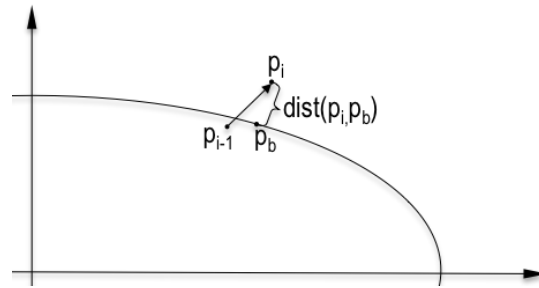
Figure 25: The closest point on the surface (p_b) may be found by minimizing the distance from the point found in iteration i (p_i) outside the ellipsoid to a point on the boundary, where the point found in iteration $i - 1$ (p_{i-1}) is used as starting value.

5 RESULTS

To evaluate the performance of the AES algorithm, it is compared to two boundary methods [17, 10] that are frontier methods for selecting test manikins. In the first test case, the manikins generated by these methods are also compared to the manikins generated by a percentile method, which is commonly used by the industry.

The algorithms are tested on cases based on assembly operations from the automotive industry. In the first test case, a protective block is placed inside a car door, whereas in the second case an electronic controlling device is placed under the driving unit, see subsections 5.3 and 5.4 respectively. The assembly paths are generated in Industrial Path Solutions [12], and are guaranteed to be collision free.

Section 1.1.1 shows how the boundary manikins are generated and the generations of percentile manikins are shown in Section 1.1.3. The AES algorithm uses an ergonomic function to select test manikins. Thus, to make comparisons with manikins generated by the other methods, the corresponding ergonomic result for these manikins when they perform the assembly operation is also calculated.

5.1 Reduction of the Anthropometric Data Set

All manikins are generated using the same anthropometric data set, and the anthropometric dimensions are adapted to the kinematical skeleton using the same regression equations. The eigenvalues of the correlation matrix are arranged according to the amount of variance captured by the corresponding eigenvector, see Figure 26 a). In the same manner, the eigenvalues for the covariance matrix are shown in Figure 26 b). Figure 26 c) shows the amount of variance captured by each eigenvectors of the correlation and the covariance matrix. Due to different units in the anthropometric data, set the correlation matrix is used. In Figure 26 a) it may be observed that there is a break of in the amount of variance captured by the eigenvectors around the first five eigenvectors. For example, by retaining these five vectors out of the 56 original corresponds to retaining 75% of the total variation.
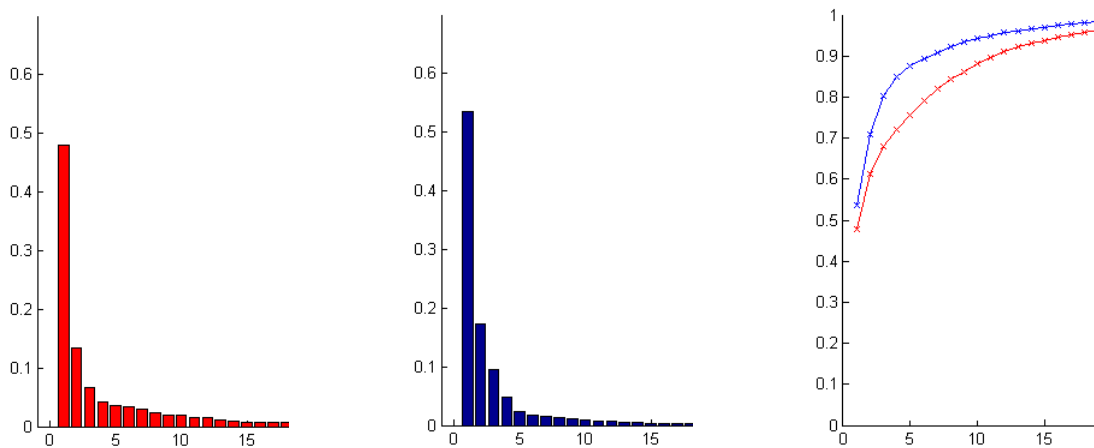
Figure 26: a) The eigenvalues of the correlation matrix arranged according to the amount of variance captured by the corresponding eigenvector. b) The eigenvalues of the covariance matrix arranged according to the amount of variance captured by the corresponding eigenvector. c) The eigenvalues of the correlation (red) and covariance (blue) matrix arranged according to the amount of variance captured by the corresponding eigenvector.

5.2 Ergonomic Criteria on an Assembly Path

The IMMA manikin tries to find as comfortable poses as possible for the manikin in each step of the path. Figure 27 shows the comfort function for five manikins that perform the assembly operation in Figure 29. Figure 28 shows a close up of the lower left region of Figure 27. The five manikins are selected to show the different shapes of the ergonomic function that usually occurred during the experiments.
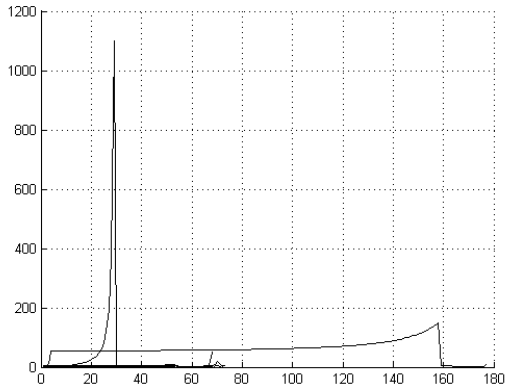
Figure 27: Shows the comfort for five manikins that perform the assembly motion in Figure 29.
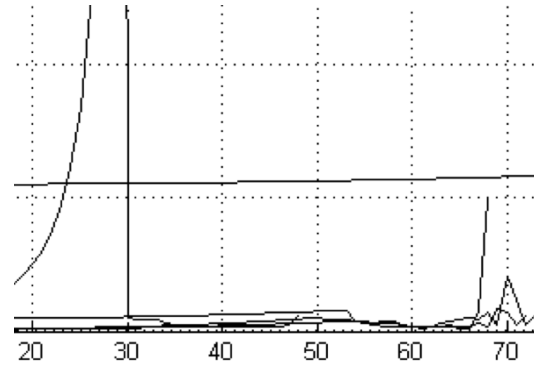
Figure 28: Shows a close up of the lower left region in Figure 27.

5.3 Test Case 1

The manikins were not allowed to move their feet during the assembly operation. However, before the manikins started to follow the assembly path they were able to move their feet and place themselves in their most comfortable position. Both hands where used to assemble the object, see Figure 29. In the following step the IMMA manikin automatically calculates poses that follows the assembly path with as good comfort as possible. Five samples of the full path are shown in Figure 29.
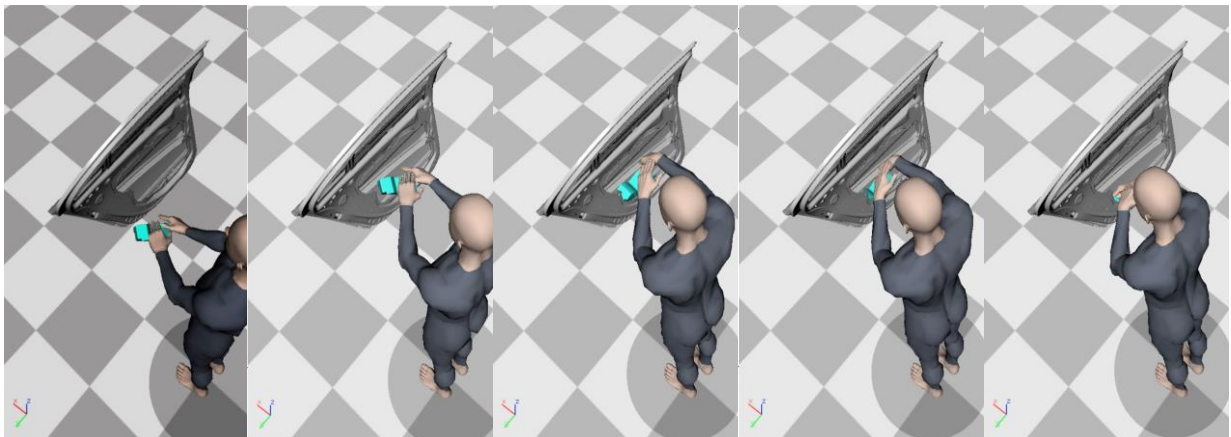
Figure 29: Show five sample of the assembly of a protective block inside a car door.

Fifteen samples were drawn by the AES algorithm in three runs where 55, 75 and 85 percent of the original data set were covered respectively. The manikins found by the AES algorithm were compared to three different setups of test manikins generated from the boundary method A presented in Section 1.1.1. The first one uses stature and weight as dependent variables, which results in four boundary and one center manikin, whereas the other two uses three additional dependent variables for creating the manikins listed in Table 2.

The three extra variables used in the two latter simulations where selected by experts in the field of assembly ergonomics. The percentile method is used in the simulation since it is commonly used in the industry today. The results from the AES algorithm, the boundary and the percentile method are shown in Table 1. The test manikins returned from the AES algorithm were further examined and they turned out to be non-boundary manikins.

Table 1: The comfort of the manikins when they perform the assembly in Figure 29. The three extra variables used to create the boundary manikins marked with 1) and 2) are shown in Table 2

Percentiles		Boundary case 2 variables	Boundary case 5 variables[1]	Boundary case 5 variables[2]	AES 2 eigenvectors	AES 5 eigenvectors	AES 9 eigenvectors
(95-p)	**704.5**	69.8	65.4	466.0	**685.2**	58.7	135.4
(5-p)	87.6	**1122.4**	85.7	65.5	60.5	111.1	320.5
		81.6	6893.2	103.7	55.6	64.6	1147.4
		100.6	17383.1	83.8	399.6	58.2	26014.1
		89.1	503.8	102.4	68.2	68.0	130.7
			127.4	**2851.3**	68.5	82.5	1396.3
			25537.7	70.1	78.2	492.4	184.4
			68.6	185.4	141.1	61.2	82.1
			265.6	1073.7	58.2	57.7	55.2
			183.3	612.3	55.1	10109.1	147.1
			105.1	1813.3	130.3	1988.2	**55178.9**
					63.3	**32306.4**	55.0
					66.6	68.4	75.5
					182.8	67.4	60.4
					62.7	705.8	82.9

Table 2: Show the three extra variables used in to create the boundary manikins marked with 1) and 2) in Table 1.

Extra variables used in 1)	Extra variables used in 2)
– Shoulder height – Iliac spine height, standing – Shoulder (bideltoid) breadth	– Sitting height – Elbow height – Hand breadth

5.4 Test Case 2

In the second test case, an electronic controlling device is placed under the driving unit of a car. Figure 30 shows for six samples of the assembly operation. The manikins were allowed to move their feet during the assembly operation. However, the manikins have to use their left hand for support to maintain the balance whereas the right hand were used to perform the assembly operation as shown in Figure 30. All manikins use the same support place for their left hand. The support place was selected by studying an average 50 weight and 50 stature percentile manikins and selected to be in the recommended workspace region [18].
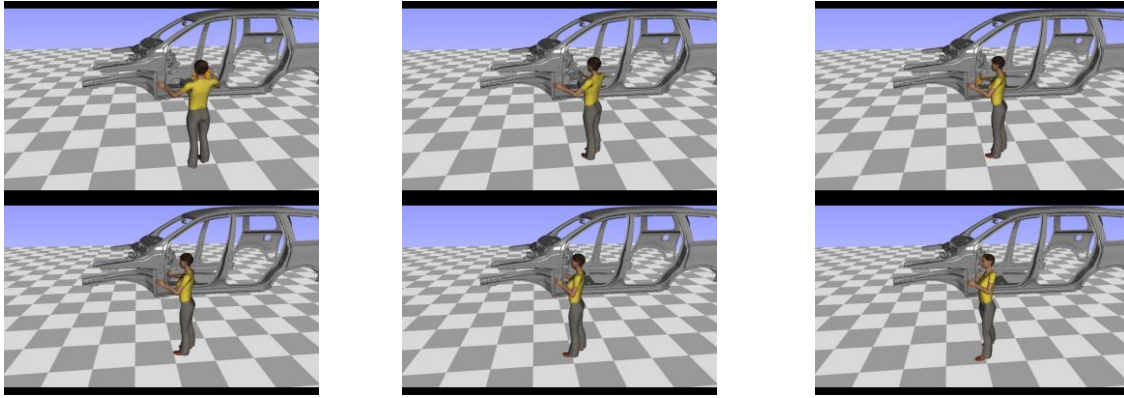
Figure 30: Shows six samples of the assembly of an electronic controlling device inside a car door.

If a manikin collides with the environment it is not possible for the manikin to further perform the assembly operation. As stated in section 4.4, when a collision occurs the assembly motion is aborted and the manikin that fails to perform the assembly operation is returned to the user as a relevant test manikin. Figure 31 shows a collision between the manikin and the car.

Figure 31: Shows a collision between the manikin and the car with (left figure) and without the manikin mesh rendered (right figure). The blue figure shows the collision model of the manikin and the red part indicates where the collision occurs.

The AES algorithm uses 15 samples and is compared to the boundary method B in Section 1.1.1. The comparisons were made using 55 and 75 percentage of the original data set. The results are shown in Table 3 and respectively. Also, the test manikins generated from the AES algorithm were further examined, and they turned out to be both boundary and non-boundary manikins.

Table 3: Shows the result for the boundary method (right) and for the AES algorithm (left) when two eigenvectors are used.

Nr	C()	Collision		Nr	C()	Collision
1	**48.0**	**Yes**		1	185.9	No
2	**179.8**	**Yes**		2	305.0	No
3	185.3	No		3	**610.1**	**Yes**
4	185.7	No		4	184.6	No
5	186.5	No		5	180.4	No
6	181.8	No		6	184.9	No
7	188.6	No		7	224.3	No
8	184.1	No		8	179.5	No
9	**305.7**	No		9	**315.5**	No
10	204.9	No				

Table 4: Shows the result for the boundary method (right) and for the AES algorithm (left) when four eigenvectors are used.

Nr	C()	Collision
1	178.1e+004	**Yes**
2	183.3e+004	**Yes**
3	214.0e+004	**Yes**
4	172.7e+004	**Yes**
5	236.3e+004	**Yes**
6	183.0e+004	**Yes**
7	177.6e+004	**Yes**
8	185.3e+004	**Yes**
9	363.6	**Yes**
10	376.5	**Yes**
11	359.6	**Yes**

Nr	C()	Collision
1	186.0	No
2	390.0	No
3	213.7	No
4	203.4	No
5	198.6	No
6	187.5	No
7	180.2	No
8	177.4	No
9	177.4	No
10	181.7	No
11	215.3	No
12	174.5	No
13	236.5	No
14	184.4	No
15	**184.4e+004**	**Yes**
16	178.3	No
17	267.6	No
18	184.0	No
19	221.9	No
20	179.6	No
21	263.1	No
22	181.1	No
23	268.7	No
24	185.7	No
25	340.0	No

5.5 Validation of the Test Cases

Additional samples were made for the AES algorithm in each assembly case to validate the result of the algorithm. In the first assembly case, an additional 100 runs of the AES algorithm were made for each reduced set. The results are shown in Table 5.

Table 5: Shows the result of a verification sampling for 100 runs of the AES algorithm for each set of eigenvalues kept in the first assembly case.

Number of eigenvectors	Samples larger then AES result
2	5
8	13
9	21

In the second assembly case, 15 and 50 extra runs of the AES algorithm were conducted for the case of two and four eigenvectors respectively. These runs converged into the same manikins that had been found by the algorithm. In the case when four eigenvectors were used an additional 25 random samples were also drawn from the hyper-ellipsoid. These samples did not contain any ergonomic results that where larger than those found by the algorithm.

6 DISCUSSION

This section is divided into subsections that covers the different areas of the AES algorithm as follows: (i) Sampling in High Dimensional Data (ii) Anthropometric data (iii) Ergonomic criteria (iv) Test cases (v) Results (vi) The AES Algorithm.

6.1 Sampling in High Dimensional Data

Even if the experiments are made on low dimensional data, it is enough to show how the increased dimensionality of a data set also increases the region of possible anthropometrical combinations. Thus, when the methods are compared with the two-dimensional data set, there are no significant differences in the resulting manikins. However, when four eigenvectors are kept there are differences among the generated manikins.

The boundary case method relies on an assumption that the manikins with the most critical ergonomics lies on the boundary see section 1.1.1 and 1.1.3. However, even if this assumption would be valid, the method still lacks in coverage. Thus, even if the samples increases with the number of eigenvectors kept, the surface of the hyper-ellipsoid to be covered by the samples increases much faster. Also, only fixed points are considered at the surface, which leads to regions on the boundary where manikins with critical ergonomic may exist. Thus, in higher dimensions, it is more likely to exist manikins with worse ergonomics than what the boundary method covers, which is also shown by the results. However, since the AES algorithm searches the set, it may still find all the manikins with worse ergonomics regardless of the dimensionality. Furthermore, it also searches the interior of the hyper ellipsoid, and thereby covers more regions compared to the boundary method.

6.2 Anthropometric Data

The anthropometric data set is normally distributed. Hence, PCA may be used to reduce the dimensionality. Also, since the data set consists of different units, the reduction is made using the correlation matrix.

It should also be taken into consideration that by reducing the data with PCA, it is assumed that high correlated data may be grouped together, and that it may answer for the majority of the variance in the data set. However, it may exist low correlated anthropometric data that have been removed during the reduction that may contribute to the ergonomic comfort.

6.3 Ergonomic Criteria

The ergonomic assessment in an assembly operation is quantified by the comfort function. A main advantage of using the comfort function is that it may be expanded to consider more ergonomic criteria. This makes the AES algorithm more flexible compared the methods currently used for generating test manikins since they usually relies on different static assumptions, such as the manikins with the largest or smallest anthropometric dimensions always will represent the extreme manikins.

The manikins that were generated by the compared methods did not show very much difference in the comfort when two eigenvectors were used. However, with the usage of more ergonomic criteria in the comfort function, the AES algorithm might generate manikins that differ more than those generated by the boundary method even in the case when two eigenvectors are used.

Even if the experiments show that there are differences in the comfort between the manikins when they perform the assembly operations, it does not imply that any manikin suffers from discomfort during the operation. Thus, one drawback of quantifying the comfort with the comfort function is to determining a limit to which says that the discomfort should be accepted or not. However, this might be covered in a future work, where the ergonomic result is compared to data which is known to cause injures and may thereby be used to determine if the comfort is good or bad [24].

6.4 Test Cases

The test cases are based on real assembly operations, and the workspaces are constructed according to recommendations of [18]. The differences in the assembly cases are enough to show the differences in the comfort for the manikin performing them.

The manikins are not allowed to move their feet during the assembly operation in the first test case. This since there is no penalty in the comfort function for moving on the floor. This lack of cost tends to make the manikin moving more on the floor instead of using the joints to follow the path. Moreover, the assembly path is chosen to ensure that it is possible for a manikin to perform the assembly simulation without moving the feet.

In the second test case the manikin are allowed to move on the floor, even if there is no penalty. However, in this assembly case, the manikins need to take more consideration of the environment. Moreover, compared to the first case, the manikins now have a longer path to follow. Thus, due to the length of the path, it is unrealistic to prevent the manikins from moving the feet.

6.5 Results

The results show that the AES algorithm finds manikins that perform the assembly operation with worse ergonomics compared with the manikins generated by the other methods. In both test cases, the AES algorithm finds manikins that either has a higher discomfort or may not be able perform the assembly operation.

The boundary method and the percentile method rely on the assumption that the critical manikins always exist at the boundary of a selected interval. However, in this work it has been shown that this assumption may not always hold, which coinciding with the experimental results in [6]. Thus, it is shown that there exist manikins in the interior with worse ergonomics than those on the boundary. It is furthermore shown that even if the manikins on the boundary may perform an assembly operation there exist manikins in the interior that cannot perform the operation.

The results in Table 2 show how the choice of selecting anthropometric variables when generating test manikins may affect the resulting manikins. Thus, the boundary method will not always generate relevant test manikins since too few or uncorrelated dependent variables may be used. Hence, knowledge of both the underlying regression equations and experience in assembly ergonomics is required to be able to generate relevant test manikins. This is not necessary when the AES algorithm is used, since all anthropometric variables are considered throughout the entire assembly operation. Furthermore, as pointed out by [25], the choice of anthropometric variables may affect the accommodation of the generated test manikins. If the user selects anthropometric dimensions to be used as dependent variables in regression equations, and if these variables are few and have a low correlation with the estimated variables, then it might result in errors in the estimations, which will result in a set of less representative test manikins [25]. The region covered by the confidence ellipsoid also increases when more variables are used to create test manikins. Thus, even if an experienced user adds more anthropometric key variables to ensure that the extremes of the anthropometric variables are covered, the expected region to be covered has at the same time been increased.

When looking at the ergonomics in each time frame, it can be seen that the comfort function has three characteristic shapes, see Figure 27. The manikins that are performing the operation with no problem have an almost linear function, whereas manikins where the function takes big steps indeed are suffering from the operation. The third shape represents manikins that only suffer from a part of the assembly operation. These graphs may be useful for evaluating were the problems occur during an assembly operation.

The result also shows that manikins may fail to perform the assembly operation due to collision with the environment. However, it may still be possible for a human to perform the assembly operation. This, since a human assembly worker may be allowed to support against objects in the environment in order to properly perform an assembly operation. However, in the current version of the IMMA program, it is not possible for a manikin to support against objects in the environment unless the user explicitly specifies the manikin to do it.

34

6.6 The AES Algorithm

The time consuming part of the AES algorithm showed to be the evaluation of the test manikins. The response surface is numerically estimated and several manikins need to be evaluated in order to build and traverse the response surface.

The choice of a using several first order functions for approximating the response surface prior to, for instance using a second ordered surface is due to the computational cost of estimating the response surfaces. It may be the case that a second order surface is insufficient, and several second order surfaces have to be computed in order to converge, which is more expensive to compute compared to several first order surfaces. As another example, consider an algorithm that starts to test if a first order surface is sufficient, and if it fails it tries to test if a second order surface might be a better choice. If the second order also fails, the algorithm iteratively tries to use a surface with a higher order until a surface that fits is found. Thus, due to the coefficients needed to compute the functions, the computational cost is increased in each iteration. Especially in higher dimensions it is cheaper to iteratively follow smaller linear segments compared to iteratively trying to fit several high order surfaces. However, only utilizing first order approximations may lead to convergence problems since it is more likely that they will get stuck in a local optimum, and more seeds are needed to ensure that all optima are found.

There exist cases when the AES algorithm tries to find the closest manikin on the boundary and fails to reach the exact point of the boundary and stops at a point close it. However, this is most likely depending on the usage of a barrier function, which may be solved by changing the method to a Lagrange multiplier or by projecting the gradient onto the boundary.

The experiments are conducted at different stages of the development of the AES algorithm. Two main differences between these experiments are that in the second experiment it is possible for the manikin to abort and report a failure if it does not succeed to perform the operation and that the weights of the comfort function have been adjusted. Also, the AES algorithm has also been improved between these experiments. In the first test case, there tended to be many points where the algorithm does not always succeed to converge, especially in the cases where more eigenvectors where used. Thus, even if some of the resulting manikins seem similar, it may be concluded that the all seeds do not converge. However, all the seeds in the second assembly case converge to manikins that have already been found.

7 CONCLUSIONS AND FUTURE WORK

The ergonomics is an important factor in the design of products and workspaces, and it has been shown that the assembly ergonomics is related to the production quality. Thus, in order to maintain a sustainable high quality production it is important evaluate the assembly ergonomics with relevant test manikins, and preferably early in the design phase of a project. However, it is far from trivial how these relevant manikins should be selected.

In this work, we have introduced a new automatic algorithm called Adaptive Ergonomic Search (AES) for selecting relevant test manikins. The algorithm is based on surface response methodology and considers the ergonomics throughout the whole assembly motion. It furthermore uses the entire set of anthropometric data to iteratively build up the set of relevant test manikins. The algorithm is compared with boundary methods and a percentile method.

The comparisons are made on assembly cases from the automotive industry and the results show that the AES algorithm generates test manikins that have worse ergonomics or may not be able to perform the assembly operation compared to the manikins that are generated by the compared methods. The results also show some of the advantages of using an automated algorithm for generating test manikins. It both eliminates the problem of identifying which anthropometric dimensions that are relevant to test, and it also adapts this set of test manikins to the investigated assembly operation. Thus, the AES algorithm is suitable for non-expert users. The algorithm also offers an adaptive evaluation since more ergonomic criteria may be included in evaluation of the comfort.

Due to the lack of cost of a manikin to move on the floor, one of the assembly simulations is made without letting the manikins moving the feet. Even if the comfort function is fairly simple and gives realistic motions in most cases, a topic for future research is to adjust the weights of the joints and to extend the comfort function by adding more ergonomic criteria, such as penalty for walking.

It would be interesting to further compare the algorithm with other methods and on more complex assembly cases. However, in such experiments, the comparisons should be carried out together with expertise in the field of assembly ergonomics to ensure a proper usage of the compared methods.

When comparing manikins, there is no defined threshold to distinguish between good and bad in terms of the comfort function. Instead the comfort is compared between all the manikins, and we say that a manikin is suffering more from an assembly motion if there is large gap in the comfort between the compared manikins. Hence, a topic of future research is to develop a better definition of what is considered as comfortable motion and what is not in terms of the comfort function.

The AES algorithm may have to generate many manikins to find a relevant set of test manikins. However, this may be improved in future work by implementing and evaluate different optimization algorithms and techniques for dimension reduction. A drawback with the algorithm is that it might be time consuming. The runtime of the algorithm is an important factor to consider in future work. This since additional functionality is constantly added to the manikin, which makes the manikin simulations more expensive to compute. Also, it is highly interesting to investigating more methods for determine the step size of the algorithm to improve the convergence. This will also reduce the runtime of the algorithm. Moreover, it may also be interesting to implement methods to prevent the algorithm to get stuck in local optima. Thus, it will reduce the number of samples needed for the algorithm, and thereby furthermore reduce the runtime.

A manikin in IMMA may be generated out of two anthropometric variables. The remaining variables are then estimated using hierarchical regression equations [17]. However, this could also be used as an alternative approach for reducing the dimensionality instead of applying PCA. A variable selection algorithm may identify which of the anthropometric variables that should be used to generate the manikins. Since the manikins are created by using regression equations, it may be possible to perform a root cause analysis, which might reveal important information about which anthropometric variables that have most influences in a certain assembly operation.

REFERENCES

[1] Y. Heecheon and R. Taebeum, "Development of hierarichial estimation method for anthropometric variables," *International Journal of Industrial Ergonomics 35,* pp. 331-343, 2005.

[2] D. Högberg, G. Bäckstrand, D. Lämkull, L. Hanson and R. Örtengren, "Industrial customisation of digital human modelling tools," *International Journal of Services Operations and Informatics,* pp. 53 - 70, 2008.

[3] R. Bohlin, "Robot Path Planning," Chalmers University of Technology, Göteborg, 2002.

[4] A.-C. Falck, R. Örtengren and D. Högberg, "The Impact of Poor Assembly Ergonomics on Product Quality: A Cost–Benefit Analysis in Car Manufacturing," vol. 20, no. 1, p. 24–41, 2010.

[5] A.-C. Falck, Virtual and Physical Methods for Efficient Ergonomics Risk Assessments - A Development Process for Application in Car Manufacturing, Göteborg: Chalmers University of Technology, 2007.

[6] H. Speyer, "On the definition and generation of optimal test samples for design problems," Human Solutions GmbH, Kaiserslautern, 1996.

[7] HFES 300 Committee, Guidelines For Using Anthropometric Data In Product Design, Santa Monica, CA: Human Factors and Ergonomics Society, 2004.

[8] L. Hanson, D. Högberg, R. Bohlin and J. Carlson, "IMMA – Intelligently Moving Manikins – Project Status 2011," Lyon, 2011.

[9] A. Bittner, "A-Cadre: Advanced family of manikins for workstation design," in *Proceedings of the IEA 2000/HFES 2000 Congress*, Santa Monica, CA, 2000.

[10] E. Bertilsson, D. Högberg, L. Hanson and Y. Wondmagegne, "Multidimensional consideration of anthropometric diversity," in *First International Symposium on Digital Human Modeling*, Lyon, 2011.

[11] D. Montgomery and R. Myers, Response surface methodology : process and product optimization using designed experiments, New York: Chichester : Wiley, cop., 2002.

[12] Fraunhofer-Chalmers Research Centre , "(IPS) Industrial Path Solutions," 2012. [Online]. Available: www.industrialpathsolutions.com.

[13] R. Bohlin, N. Delfs, L. Hanson, D. Högberg and J. Carlson, "Unified solution of manikin physics and positioning - Exterior root by introduction of extra parameters," in *First International Symposium on Digital Human Modeling*, Lyon, 2011.

[14] Microsoft, "Visual Studio," 30 09 2012. [Online]. Available: http://www.microsoft.com/visualstudio/eng/team-foundation-service. [Accessed 30 09 2012].

[15] N. Delfs, "Manikin in Time; Development of a Virtual Manikin with Inverse Kinematics and Comfort," in *velopment of a Virtual Manikin with Inverse Kinematics and Comfort. Master Thesis. Department of Mathematical Sciences*, Göteborg, 2011.

[16] L. Hanson, S. L., G. Gard, S. Ipsen and C. Vegara, "Swedish anthropometrics for product and workplace design," *Applied Ergonomics,* vol. 40, no. 4, pp. 797-806, 2009.

[17] E. Bertilsson, L. Hanson, D. Högberg and I.-M. Rhén, "Creation of the IMMA manikin with consideration of anthropometric diversity," Stuttgart, 2011a.

[18] J. Roebuck, K. H. E. Kroemer and W. Thomson, Engineering anthropometry methods, New York: Wiley-Interscience, cop, 1975.

[19] H. Gatignon, Statistical Analysis of Management Data, New York: Springer , 2010.

[20] I. Jolliffe, Principal Component Analysis, 2nd ed., New York: Springer-Verlag, 2002.

[21] P. Glasserman, Monte Carlo methods in financial engineering, New York: Springer, 2004.

[22] J. Lundgren, M. Rönnqvist and P. Värbrand, Optimeringslära, Lund: Studentlitteratur, 2010.

[23] B. Husslage, G. Rennen, E. van Dam and D. den Hertog, "Space-filling Latin hypercube designs for computer experiments," *Optimization and Engineering,* vol. 12, no. 4, pp. 611-630, 2011.

[24] K. A., D. Högberg, L. Hanson, D. Lämkull, N. Delfs, I. Rhen and R. Örtengren, "Ergonomic Risk Assessment of a Manikin's Wrist Movements - a Test Study in Manual Assembly," in *Second International Symposium on Digital Human Modeling*, Ann Arbour, 2013.

[25] H. You and T. Ruy, "Development of hierarichial estimation method for anthropometric variables," *International Journal of Industrial Ergonomics, 35,* pp. 331-343, 2005.

APPENDIX A: LIBRARIES AND CONTACT INFOMATION

The algorithm is implemented in C++, which is the default language used in the IMMA project. Table 6 lists the libraries used together with their reference. Table 2 contains the contact information.

Table 6: The libraries used in the implementation.

BOOST	http://www.boost.org/
Armadillo C++ linear algebra library	http://arma.sourceforge.net/
FCC Standard library[1]	http://www.fcc.chalmers.se/

Table 7: Contact information.

Erik Brolin	erik.brolin@his.se
Lars Hanson	lars.hanson@scania.com
Dan Högberg	dan.hogberg@his.se

---

[1] This library is only intended to be used in FCC's software and, hence it is not available for public use.